The Chemical Engineering Journal, 23 (1982) 105 - 108

Short Communication

Use of the Stefan cell to obtain solvent diffusivities

JAMES M. POMMERSHEIM, JAMES T. SEELEY and JESSE VAN KIRK

Bucknell University, Lewisburg, PA 17837 (U.S.A.)

(Received 14 April 1980; in final form 5 January 1981)

The Stefan cell consists primarily of a narrow glass or metal tube containing an evaporation solvent. Air or other inert gas is passed across the open top of the cell. Because of the concentration gradient established between the surface of the liquid and the cell top, solvent evaporates and the liquid level drops.

The use of the Stefan cell has become a simple and reliable means of determining gaseous diffusion coefficients of evaporating solvents. In earlier studies discontinuous methods of determining the amount of solvent evaporated based on weight or volume measurements were employed [1, 2]. Continuous experimental methods based on the detection of changes in liquid interface levels have been shown to be potentially superior [3]. The major advantage of the continuous method of data collection is the fact that many data points (interface level, time) can be collected from a single run. In our studies we have been mainly concerned with perfecting the continuous method by achieving precisely controlled experimental conditions of temperature, pressure, flow rate and cell geometry. We describe here a convenient method of using interface data obtained from the Stefan cell to determine solvent diffusivities and also show what effects changing cell geometry and flow rates have on the value of the diffusion coefficient.

Theory

A schematic of the basic Stefan diffusion cell containing a pure liquid A is shown in Fig. 1 (insert). Inert gas B is swept across the top of the cell to remove the evaporating vapors of liquid A. Ideally the whole system is maintained at a constant temperature, pressure and flow rate. As A evaporates it first diffuses through a path of stagnant vapor above the liquid before mixing with pure gas B at the top of the cell. Depending on the flow velocity of the inert gas there, two different mixing effects may occur. These effects cause the actual diffusion path length to differ from the physically measured path length by a correction factor, ΔZ. If this factor is subtracted from the measured diffusion path length a value for the actual path length results. At high gas velocities turbulent eddies form at the top of the cell which partially destroy the stagnant film. This causes a

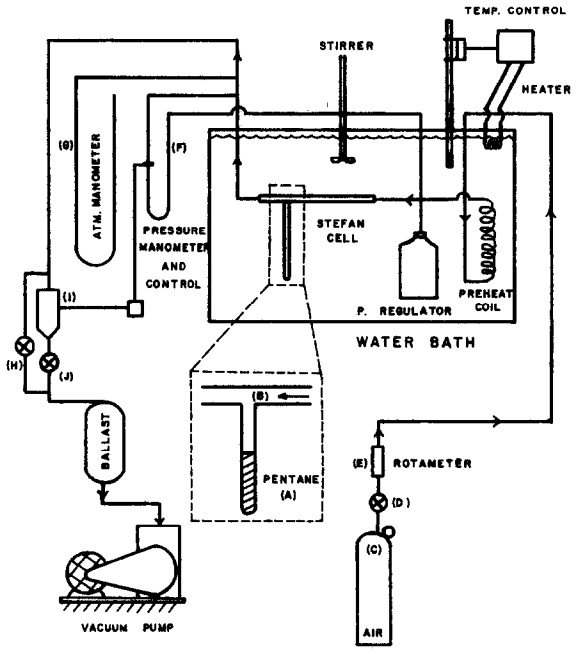

Fig. 1. Schematic of experimental apparatus (insert - Stefan cell).

mixing well of depth ΔZ to form, decreasing the actual path length. On the other hand, at sufficiently low gas velocities, poor mixing results and a plume of solvent vapor extending above the cell forms. This results in an increased actual path length for diffusion.

Experimental measurements consist of the interface depth Z_i (measured from the top of the capillary tube) at time t. The initial interface depth is Z_1 at $t = 0$. Presuming constant total pressure and solvent partial pressure at the top of the cell, Pommersheim and Ranck [3] have shown that

$$Y/2 = \frac{D_{AB}}{\rho_1 RT}\,\frac{t}{Y}\,\ln\left(\frac{P - P_{A0}}{P - P_A^0}\right) - (Z_1 - \Delta Z) \quad (1)$$

$Y = Z_i - Z_1$ is the total drop in interface depth. If the inert gas B is free of solvent A then the partial pressure of A at the cell top P_{A0} is zero.

A plot of $Y/2$ *vs.* t/Y linearizes this equation. The slope and intercept of the linearization yield experimental values for D_{AB} and ΔZ, respectively. One important point to note is that the path length correction factor is separated in the equation from the diffusion coefficient, thereby separating the errors associated with each respective value when statistical analyses are performed on the data.

Apparatus

The apparatus used in determining values for D_{AB} and ΔZ was an improved version similar to the one originally used by Pommersheim and Ranck [3]. The system (see Fig. 1) was designed to maintain a precise pressure control (±1 mm Hg), temperature control (±0.01 °C), and flow rate control (±3 ml/min). The option to change cell vessel geometry was also available.

The system pressure was maintained at 760 mm Hg using an I^2R Man-o-Watch (Model No. MW-1), a photosensitive control device. This device regulates the pressure of a closed system by sensing the change in mercury level of an attached closed manometer. We adapted the control device so that it would be capable of controlling the pressure accurately for a flow system rather than for a batch system. In order to enable better pressure control, a mixture of dye and water was used in place of mercury. The pressure control operated as follows: Air (dry, high purity) was bled from gas cylinder C into the system. Flow rates were controlled by inlet needle valve D and measured with a calibrated rotameter E. The dry air passed into the preheat coil and through the top of the Stefan cell. Sidelines of the exiting stream were connected to an atmospheric water manometer G and a control manometer F. Manometer G was open to the atmosphere so that the system pressure could be read in conjunction with a barometer. The other side of manometer F was attached to a constant pressure source which consisted of a one gallon glass jar submerged in the constant temperature water bath. Any change in system pressure would be reflected in a change in the level of the fluid in F which would be sensed by the pressure control device. The exiting gas passed through a parallel combination of valves H, I and J and into a vacuum pump (Sargeant–Welsch, Model No. M-1402) which served as a constant pressure sink for the exiting gases. Valve H, a highly sensitive Edwards needle valve (model LB1B), could be adjusted so that the system pressure would rise slowly as more dry air was admitted into the system than could be evacuated. The pressure would continue to rise until the control device sensed the rise in the fluid level in manometer F. When this occurred, the closed solenoid valve I would open allowing more dry air to pass from the system through valve J. The system pressure would fall and valve I would close. This cycle repeated itself so that the system pressure would slowly and continuously rise then fall between a set range of limits. By careful adjustment of valves H and J, these limits were made to fall within ±1 mm Hg. The system was completely isolated from ambient pressure changes.

Temperature control

A 25 ft. gas pre-heat copper coil, the Stefan cell, and the constant pressure bottle used for the pressure control were submerged in a well-mixed water bath maintained at a constant temperature of 31.40 ± 0.01 °C. The temperature was controlled by an I^2R Therm-o-Watch (model L7-800). This device controls a temperature bath by measuring the change in capacitance of a thermometer as the mercury level changes. We used a Fisher ASTM bomb calorimeter thermometer (Model No. 04361) and were able to achieve temperature control

within a hundredth of a degree over the entire course of a run.

Cell design

The basic Stefan cell unit (see Fig. 1 — insert) was a precision, constant bore glass capillary tube fitted into a cylindrical plexiglass vessel with a removable lid. The whole unit was submersible and air tight. The glass capillary was 23.7 cm long, had an I.D. of 0.205 cm and an O.D. of 0.780 cm, while the plexiglass vessel had an I.D. of 7.6 cm and a height of 7.0 cm. The unit geometry (see Fig. 2) was changed by varying the position of the capillary, altering the position of the gas input line, and adding a flow straightening device (consisted of 16 parallel plastic tubes within the 1/2 inch feed tubing). Figure 2 depicts the different cell geometries employed in our studies. Cell configurations A and B involved air entering and exiting from the lower part of the cell while configurations C and D had air entering from the top and exiting from the bottom. The gas input and exit lines were attached to the vessel 0.2 cm from the bottom with or without a flow straightener and the capillary was either flush with the interior bottom of the vessel (configurations B and C) or protruding upward 5.1 cm (73%) from the interior bottom (A and D). For some experimental runs, the gas input line and flow straightener were also moved to 0.7 cm from the top of the cell with the capillary being in either the protruding or flush position and the exit line remaining on the bottom. The input line did not extend into the cell when it was at the top of the cell as it did when it was at the bottom.

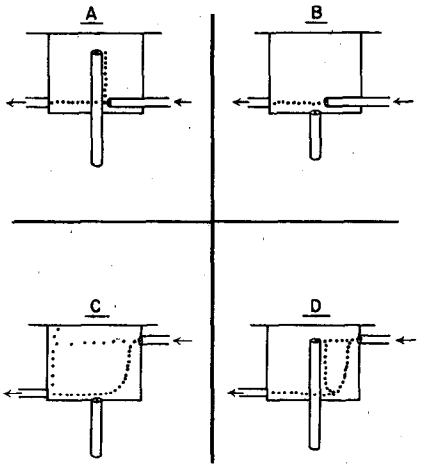

Fig. 2. Stefan cell configurations.

Experimental

The liquids used in this study were spectrograde n-pentane and spectrograde methanol. The carrier gas in both cases was high purity dry air. All runs were carried out at 31.40 ± 0.01 °C and 760 ± 1 mm Hg. The change in interface height was found using a cathetometer which could be read to a precision of 0.001 cm. Flow rates used were 20, 40 and 88 ml/min. The geometry of the diffusion cell varied from run to run. For each run only one change occurred, either a geometry change or a flow rate change. The average duration of each run was approximately 40 hours. During a run, time, interface level, temperature, flow rates, and manometer levels were recorded continually approximately every 1/2 hour, and later every hour or longer as the evaporation rates decreased.

Results

The molecular diffusion coefficients and end length correction factors for the n-pentane–air, methanol–air systems were calculated from interface level-time data using eqn. (1). The values for D_{AB} and ΔZ were determined from the best least-squares slope and intercept, respectively. All values needed for evaluating the equation except for the molar density of n-pentane were taken from the literature. The value for the molar density of n-pentane was determined experimentally using a pycnometer.

The derivation of the equation used in this analysis presumes that quasi-steady-state has been reached. Calculations based on an unsteady state Fickian model showed that for all runs, quasi-steady-state was reached (99% of equilibrium) within the first minute, so that the unsteady state start-up of the experiments did not affect the results. Also, an advantage of the method of analysis is that any time after the start of the run can be chosen as the initial time ($t = 0$). This allows the initial unsteady state data points to be disregarded.

The results of the runs indicated that the calculated values of D_{AB} were independent of the cell geometries and the flow rates used. Data from a typical run are plotted in Fig. 3. For all runs good linearity resulted, with no

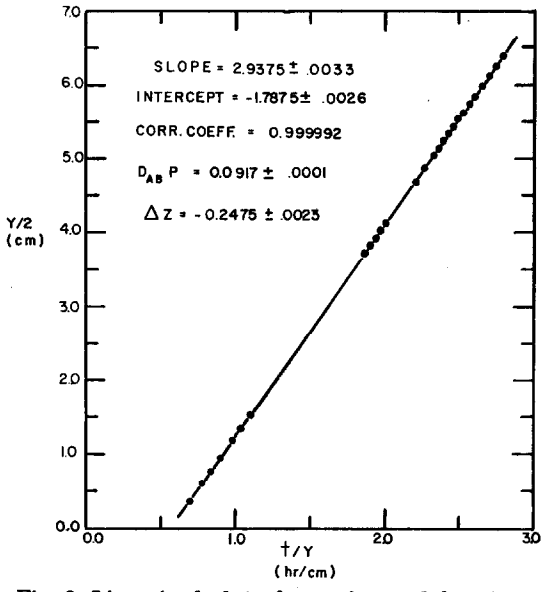

Fig. 3. Linearized plot of experimental data (n-pentane/air).

trending of the lines. Correlation coefficients were of the order of 0.9999. The first two dry-air pentane runs were carried out under exactly the same conditions to check on the reproducibility of the data. Closely corresponding values were obtained (0.0929 ± 0.0003 and 0.0927 ± 0.0002 cm^2/s. For both runs the protruding cell configuration (see Fig. 2-A) was used with a flow rate of 40 ml/min.

The addition of a flow straightener to this system made no significant change in the value of D_{AB} (0.0928 ± 0.0004). Changing the flow rate of dry air over the n-pentane from 40 ml/min to 20 and 88 ml/min also made no significant change (values of 0.0927 ± 0.0004 and 0.0920 ± 0.0006, respectively, were obtained at 20 and 88 ml/min). Next the Stefan cell was lowered so that it was flush with the bottom of the vessel and at the same level as the entering dry air flow (see Fig. 2-B). A slight (1%) decrease in the value of D_{AB} (to 0.0916 ± 0.0004) was noted. The last two runs were carried out with the dry air entering from the top of the cell rather than the bottom, (see Fig. 2-C and D). In the case where the capillary remained flush with the bottom (C), a significant lowering of the value of D_{AB} (to 0.0903 ± 0.0005) resulted. However, when the capillary was raised to the same level as the gas entrance (D), the value of D_{AB} increased to its former levels (0.0917 ± 0.0001). An average value of 0.0920 cm^2/s with a standard deviation of 0.0009 resulted from the nine pentane runs made.

This value is in close agreement with another independent researcher, Nagasaka [4]. He obtained a diffusivity for pentane–air of 0.0877 ± 0.0002 cm^2/s at 25 °C. Correcting this value to 31.40 °C using the temperature exponent given by Nagasaka gives a diffusivity of 0.0913 cm^2/s at 31.40 °C and 760 mm Hg which is well within our experimental range. The average also agrees with the value (0.0913 ± 0.0008) obtained by Pommersheim and Ranck [3] at 31.4 °C for the pentane–nitrogen system. For the pentane–air system at the same conditions this experimental diffusivity scales down to 0.0905 cm^2/s. However, they did not conduct their runs at constant pressure, so that the diffusivity is based on an average or mean system pressure. They found a fairly wide range of theoretical values for the pentane diffusivity, values which were sensitive functions of the intermolecular force constants used in their calculation.

Two runs were made using a dry air–methanol system. The resulting values for the diffusivities for a flush and protruding cell configuration at a flow of 40 ml/min, 760 mm Hg pressure, a temperature of 31.40 °C and pressure of 1 atm were 0.1618 ± 0.0034 and 0.1597 ± 0.0006 cm^2/s respectively. These values compare very well with the experimental value reported by Reid and Sherwood [5] (0.1604 cm^2/s). They compare less favorably with the values 0.191 (at 35 °C) and 0.195 (at 55 °C) cm^2/s reported, respectively, by Getzinger and Wilke [6] and Mrazek [7]. Correcting those diffusivities to 31.4 °C using the $T^{1.8}$ scaling rule given by Nagasaka [4] yields 0.1870 and 0.1705 cm^2/s, respectively.

The effect of geometry on the end length correction factor ΔZ was also investigated. It was found that the position of both the capillary and the dry gas entrance within the vessel affected the end length correction. Greater negative values of ΔZ resulted for configuration (A) than for (B) of Fig. 2. For A and B average values of −0.20 ± 0.03 cm and −0.04 ± 0.04, respectively, resulted for the pentane system, and −0.02 ± 0.005 cm and +0.15 ± 0.006 cm, respectively, resulted for the methanol system. A value of +0.30 ±

0.007 cm resulted for the pentane system with cell configuration C, while a value of −0.25 ± 0.002 cm resulted with D. The error bands on ΔZ are at least ten times smaller than those found using the apparatus of Pommersheim and Ranck [3].

These results are consistent with an interpretation based on cell turbulence or mixing well formation at high inert gas velocities (positive ΔZ) and pluming at low velocities (negative ΔZ). It should be noted that the magnitude of the ΔZ values are much smaller than the dimensions of the cell. Thus configurations A and D seem to exhibit more of a plume effect with their larger negative values for ΔZ than do B and C. The positive value for C indicates a mixing well effect.

Conclusions

Our experimental design has been shown to be capable of accurately and precisely measuring the diffusion coefficient of evaporating solvents in a Stefan cell under controlled conditions of pressure, flow rate and temperature. The system was completely isolated from its surroundings.

Within experimental error, diffusivities were found to be independent of the cell geometries and inert gas flow rates (from 20 to 88 ml/min) used.

End length correction factors were found to be dependent on the flow rate and geometry in a manner which is consistent with mixing effects at the cell top. Errors in the end length correction factor were at least an order of magnitude lower than values previously reported.

The average value for D_{AB} for the dry air–n-pentane system at 760 mm Hg and 31.40 °C was found to be 0.0920 ± 0.0009 cm^2/s. Using a dry-air–methanol system an average value of 0.1608 cm^2/s resulted. These values are in agreement with values reported elsewhere.

Nomenclature

A	evaporating liquid
B	inert gas
D_{AB}	molecular diffusivity of A in B, cm^2/s
P	total pressure, atm
P_A^0	vapor pressure of A
P_{A0}	partial pressure of A
R	universal gas constant
t	time, s
T	absolute temperature, K
Y	total drop in interface depth, cm $Z_i - Z_1$, cm
Z_i	interface depth, cm
Z_1	initial interface depth
ΔZ	end length correction factor, cm

Greek symbols

ρ_1	liquid molar density of A, $moles/cm^3$

References

1 C. Y. Lee and C. R. Wilke, *Ind. Eng. Chem., 46* (1954) 2381.
2 A. P. Altshuller and I. R. Cohen, *Anal. Chem., 32* (1960) 802.
3 J. M. Pommersheim and B. A. Ranck, *I & E C Funds 12* (1973) 246.
4 M. Nagasaka, *J. Chem. Eng. Data 18 (4)* (1973) 388.
5 R. C. Reid and A. E. Sherwood, *The Properties of Gases and Liquids*, McGraw-Hill, New York, 1958.
6 R. W. Getzinger and C. R. Wilke, *AIChE J., 13* (1967) 577.
7 R. V. Mrazek, C. E. Wilks and K. N. S. Prahu, *J. Chem. Eng. Data, 13* (1968) 508.